

Measurement of sulphuric acid aerosols in still air

April 14, 1997

Author: Alistair McIntyre

Supervision: Ir. W. Oostra
Ir. D. Verkoeijen
Dr. Ir. J.C.M. Marijnissen
Drs. H.G. Merkus
Prof. B. Scarlett M.Sc.

Abstract

It is believed that sulphuric acid is a carcinogenic substance and thus it is extremely important to be able to measure its concentration in still air accurately. Previous work has produced a monitor which operated in flowing air conditions and designed a sampling probe for still air.

By recreating the still air conditions, the funnels suitability is tested experimentally and the optimum impinger flow rate to operate under is determined. Three different setups were designed and built. The sampling performance of the probe is investigated by spraying sulphuric acid, sampling the aerosol with an impinger (type design IIR) and detecting the acid using titration.

The first setup was unsuccessful and required modifying to the second, working setup before any measurements of acid concentration could be obtained. These results were inconclusive as each impinger flow rate showed a variety of transfer efficiencies. What the working setup showed though was that the sampling probe can sample successfully in still air and that the acid lost during experiment is constant.

A final setup is used to find the flow rate which gives the maximum transfer efficiency. Here it is clearer that there is a maximum transfer efficiency of 50 %. The optimum sampling conditions to achieve this are an impinger flow rate between $8.5 - 10 \text{ l} \cdot \text{min}^{-1}$ and an impinger volume of 50 ml over a sampling period of five minutes. With this setup it is possible to achieve a minimum detectable concentration between $19 - 22.5 \mu\text{g} \cdot \text{m}^{-3}$.

Contents

Abstract	1
Table of Symbols	3
1 Introduction	5
2 Apparatus	6
2.1 Development of experimental setup	6
2.1.1 Original setup	6
2.1.2 Working setup	7
2.1.3 Final setup	7
2.2 Experimental procedure	9
2.2.1 Still air experiments	9
2.2.2 Titration with sodium hydroxide	10
3 Measurements	11
3.1 Theory of measurements	11
3.1.1 Titration with sodium hydroxide	11
3.2 Calculation of the minimum detectable concentration	13
4 Results	15
4.1 Expected results	15
4.2 Original setup	15
4.3 Working setup	15
4.3.1 Differing impinger flow rate	15
4.3.2 Small diameter pipe	17
4.3.3 Acid loss in pipeline	18
4.4 Final setup	19

5 Growth	21
6 Conclusions	22
7 Recommendations	23
A Example Calculations	25
A.1 Titration experiments	25
A.1.1 Impinger sample	25
A.1.2 Acid loss sample	26
B Calculation of the minimum detectable concentration	28
C Growth	29
C.1 Introduction	29
C.2 Theory	29
C.2.1 Water concentration in the air	30
C.2.2 Calculation of equilibrium acid concentration in the droplet	31
C.2.3 Calculation of growth factor	32
C.2.4 Calculation of growth time	33
C.3 Experiments	34
C.3.1 Experimental setup	34
C.3.2 Experimental procedure	34
C.4 Results and discussion	36
C.5 Conclusions	38

Table of Symbols

A	droplet surface area	$[\text{m}^2]$
C_0	initial sulphuric acid concentration	$[\text{wt}\%]$
$C_{H_2O,bl}$	water concentration in 'boundary layer'	$[\text{kg} \cdot \text{m}^{-3}]$
C_d	sulphuric acid concentration in droplet	$[\text{wt}\%]$
C_{eq}	sulphuric acid equilibrium concentration	$[\text{wt}\%]$
C_{H_2O}	water concentration	$[\text{kg} \cdot \text{m}^{-3}]$
C_{imp}	sampled mass concentration of 20 wt% acid	$[\text{g} \cdot \text{m}^{-3}]$
C_{md}	minimum detectable concentration	$[\text{g} \cdot \text{m}^{-3}]$
C_{neb}	output concentration of the nebuliser	$[\text{g} \cdot \text{m}^{-3}]$
C_{titre}	sodium hydroxide concentration titer	$[\text{mol} \cdot \text{l}^{-1}]$
d_{p0}	initial particle diameter	$[\text{m}]$
d_{p1}	particle diameter after growth	$[\text{m}]$
d_p	droplet diameter	$[\text{m}]$
D	diffusion coefficient of water in air	$[\text{m}^2 \cdot \text{s}^{-1}]$
f_g	growth factor	$[-]$
$\phi_{V,imp}$	impinger flow rate	$[\text{m}^3 \cdot \text{s}^{-1}]$
ΔV	flow rate through the nebuliser	$[\text{m}^3 \cdot \text{s}^{-1}]$
\mathcal{H}_0	humidity of saturated gas	$[\text{kg} \cdot \text{kg}^{-1}]$
η_{ta}	adjusted transfer efficiency	$[-]$
η_t	transfer efficiency	$[-]$
\mathcal{H}	humidity	$[\text{kg} \cdot \text{kg}^{-1}]$
$K_{HSO_4^-}$	dissociation constant	$[-]$
k	mass transfer coefficient	$[\text{m} \cdot \text{s}^{-1}]$
M_{acid}	molecular mass of pure sulphuric acid	$[\text{g} \cdot \text{mol}^{-1}]$
M_{air}	molecular mass of air	$[\text{kg} \cdot \text{mol}^{-1}]$
$m_{H_2SO_4}$	mass of sulphuric acid	$[\text{g}]$
M_{pipe}	mass of 20wt% acid within pipeline	$[\text{g}]$
M_w	molecular mass of water	$[\text{kg} \cdot \text{mol}^{-1}]$

Δm	mass difference	[g]
$n_{H_2SO_4}$	amount of pure acid sampled	[mol]
P_{w0}	saturated partial vapor pressure	[Pa]
P_w	partial vapor pressure	[Pa]
P	pressure	[Pa]
ρ_{air}	density of dry air	[kg · m ⁻³]
ρ_a	density of sulphuric acid	[kg · m ⁻³]
ρ_d	droplet density	[kg · m ⁻³]
Re	Reynolds number	[-]
R	universal gas constant	8.314 J · mol ⁻¹ · K ⁻¹
ρ_w	density of water	[kg · m ⁻³]
RH	percentage relative humidity	[%]
Sc	Schmidt number	[-]
Sh	Sherwood number	[-]
t_g	growth time	[s]
t	time	[s]
T	temperature	[K]
t_m	measuring time	[s]
$V_{0,tot}$	total volume	[m ³]
$V_{1,a}$	volume of sulphuric acid after growth	[m ³]
$V_{1,tot}$	total volume after growth	[m ³]
V_{imp}	impinger volume	[l]
V_{NaOH}	sodium hydroxide added	[l]
$V_{0,a}$	volume of sulphuric acid	[m ³]
V_s	volume of the batch sample	[l]
V	droplet volume	[m ³]
x	concentration of H ₃ O ⁺ , HSO ₄ ⁻	[mol · l ⁻¹]
y	concentration of H ₃ O ⁺ , SO ₄ ²⁻	[mol · l ⁻¹]

Chapter 1

Introduction

It is suspected that sulphuric acid is carcinogenic and in a previous study a sulphuric acid aerosol monitor has been built to measure the concentration of the acid in flowing air.

In an actual spinning plant the conditions are close to still air and therefore a sulphuric acid aerosol monitor would have to be able to sample under these conditions. In this previous study, a sampling funnel has been designed to sample in still air but has not been tested experimentally. The aim of this project is to recreate the spinning plant conditions within the lab and to verify whether or not the sampling funnel is suitable for sampling from still air.

To test the performance of the sampling funnel, several factors have to be considered. The transfer efficiency is related to the flow rate of the impinger. It must be known therefore what is the optimum flow rate to operate at.

Chapter 2

Apparatus

2.1 Development of experimental setup

2.1.1 Original setup

The overall efficiency of an experimental setup is a combination of different efficiencies. So when developing the setup, it must be clear which efficiency is being measured. For this project the one of real interest is the transfer efficiency. It describes how efficiently particles which have reached the impinger sampling tube will be collected in the liquid. For this to be possible the original experimental setup to determine the transfer efficiency at different impinger flow rates is illustrated in Figure 2.1.

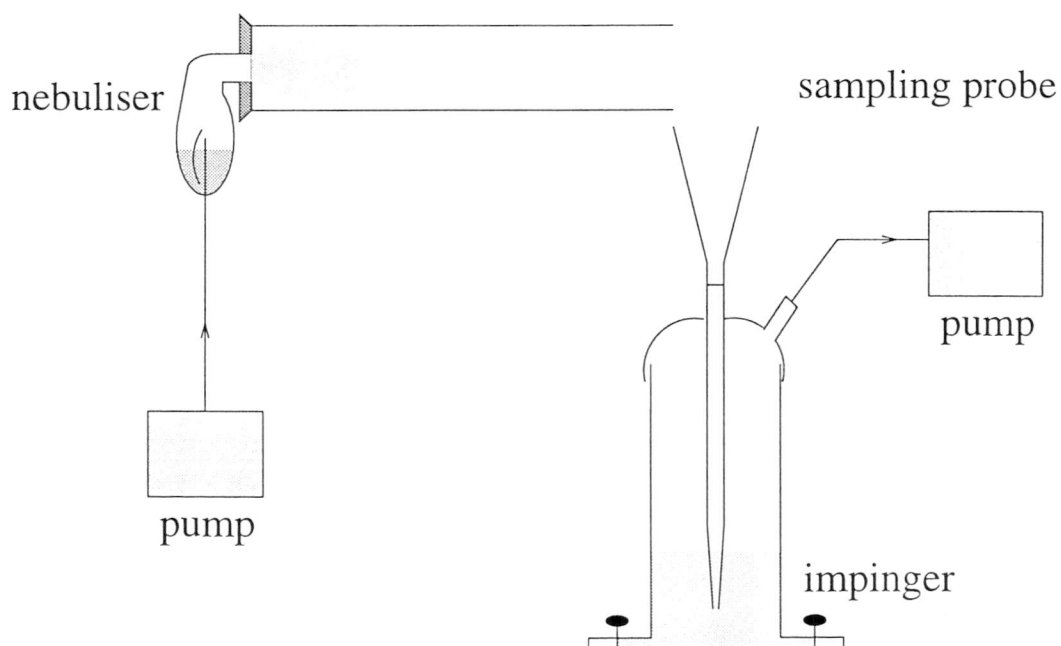


Figure 2.1: Original experimental setup

A De Vilbiss nebuliser is filled with a solution of sulphuric acid. The aerosol which is formed is sprayed into a PVC tube with a diameter of 125 mm. The mechanism used to sample the aerosol is impaction. To achieve impaction the flow is accelerated in a nozzle and the direction of flow then changed. Particles which have a high enough inertia can not follow the flow and impact on a collection plate or a fluid surface. This is performed by an impinger. Several types of impingers are available. For this project impinger type designIIr was chosen, as referring to (Verkoeijen (1997)) this was the impinger which gave the maximum transfer efficiency for laminar flow sampling. The impinger is filled with a known amount of distilled water and the water surface acts as the collection plate for the impaction. The flow rate through the impinger is adjustable to a maximum of approximately $19 \text{ l} \cdot \text{min}^{-1}$. Although the best operating range is from $7 - 12 \text{ l} \cdot \text{min}^{-1}$ and all experiments in this project are performed within this range. The sampling probe attached to the impinger was designed for sampling in still air. Figure 2.2 shows the design of the still air sampling probe used.

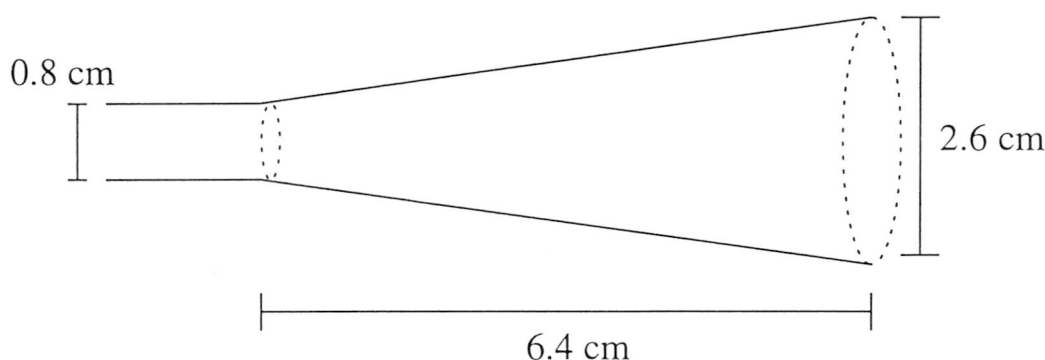


Figure 2.2: Design of funnel-shaped sampling probe

2.1.2 Working setup

With the original setup the majority of the aerosol went unsampled because there was no way of preventing the aerosol from rising up the fume cupboard before sampling could be achieved. This means that the apparatus requires adjusting to counteract this problem. Therefore a 90° bend was situated at the end of the pipe at approximately 1 m from the nebuliser outlet. This forced the aerosol downwards into the impinger. At first the impinger was positioned at the end of the bend but to improve the amount of acid caught by the impinger, it was introduced deeper into the bend. This new setup is illustrated in Figure 2.3

2.1.3 Final setup

When using the working setup, the efficiencies achieved at each flow rate showed great scatter and therefore difficult to draw any conclusions to whether there is an optimum flow rate with which the maximum transfer efficiency occurs. When there is a bend in the

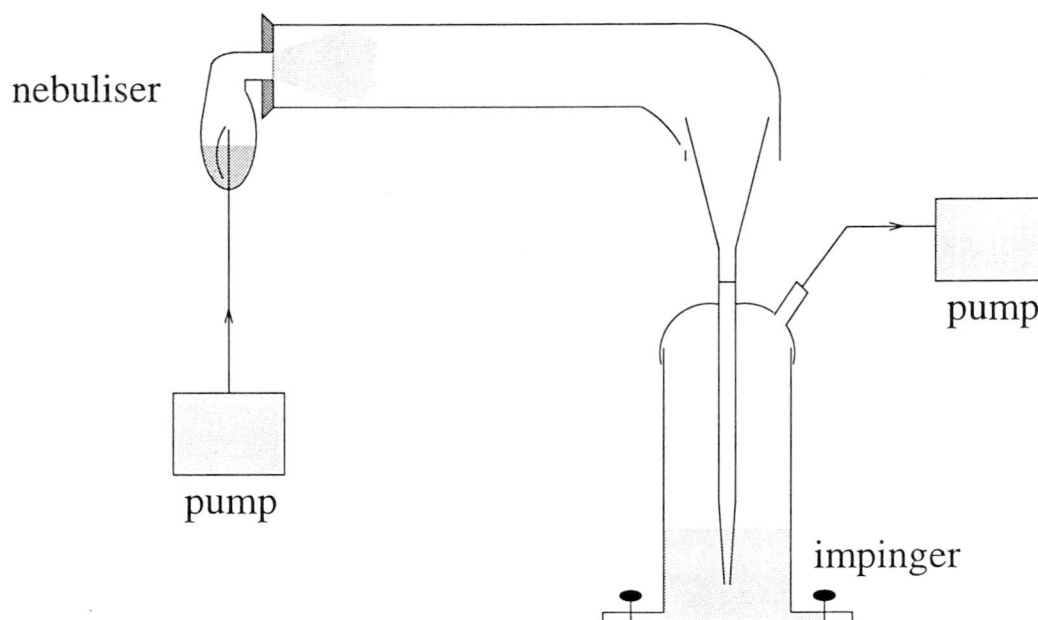


Figure 2.3: Working experimental setup

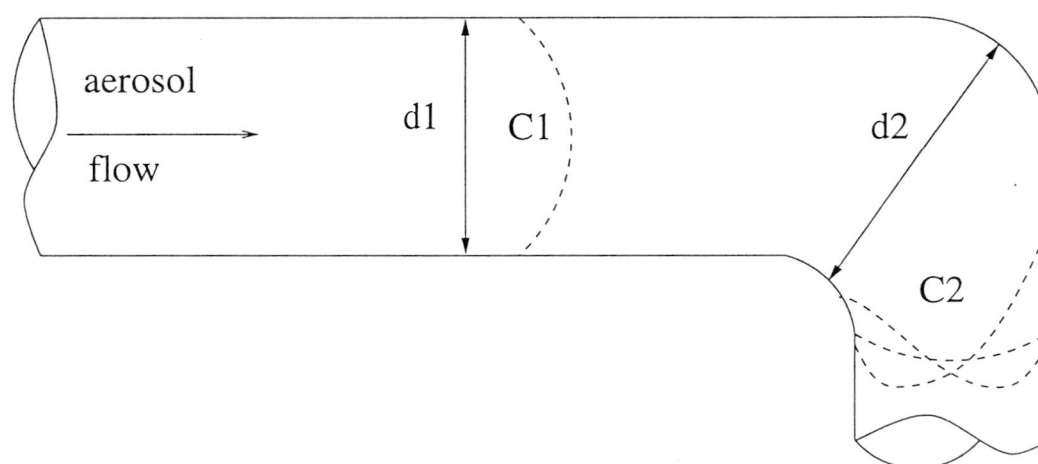


Figure 2.4: Concentration profiles of aerosol within the pipe

pipeline one should move between 10 - 20 diameters distance away from the bend before any measurements are recorded as the situation illustrated in Figure 2.4 occurs otherwise:

As $d_2 > d_1$ then C_2 could have a variety of profiles compared with C_1 , as shown. Therefore it is not known which concentration profile will be sampled. The previous setup requires the sampling probe to be placed in this area, at a distance of less than 10 diameters and this maybe the reason for the scatter in the results. Looking at the above diagram, the ideal position for the sampling probe would be at C_1 , where the concentration profile is constant. To sample here the bend was replaced with a T-junction. Figure 2.5 shows that now the impinger is inserted into the pipe at about three-quarters of the way along the pipe and thus negating any problems of a bend.

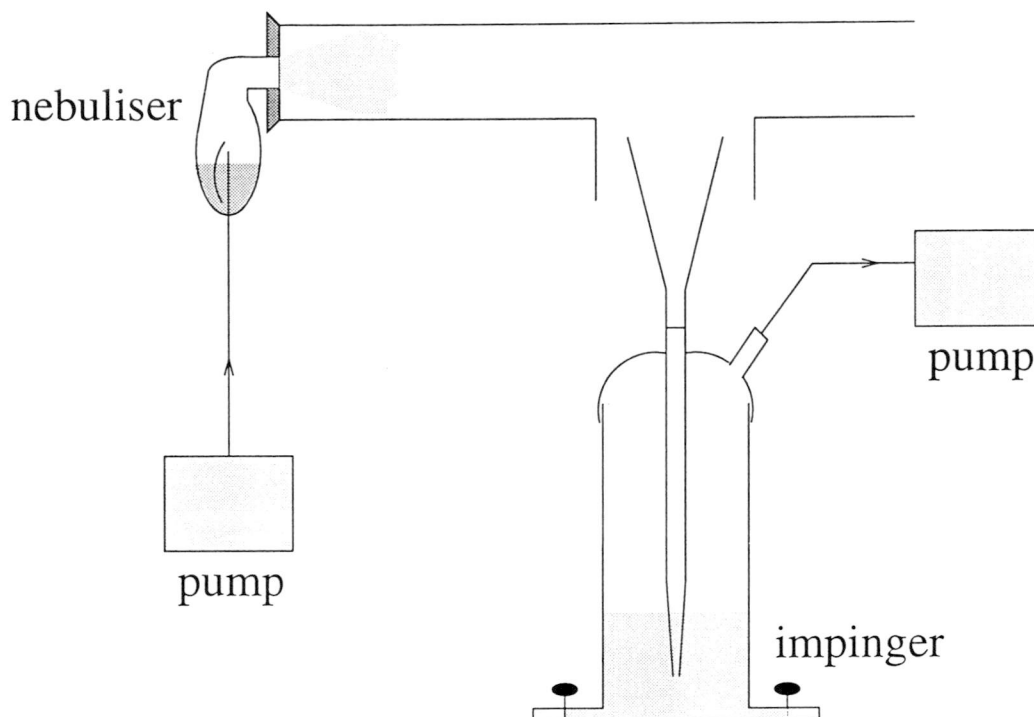


Figure 2.5: Final experimental setup

2.2 Experimental procedure

2.2.1 Still air experiments

For the still air experiments, the following equipment is used:

- MKS Mass flow meter 0258CC-10000SV (0 to $10 \text{ l} \cdot \text{min}^{-1}$)
- gas meter
- impinger type designIIr
- still air sampling probe
- pumps for the nebuliser and for the impinger

For different impinger flow rates the same experiment is performed. The nebuliser is filled with a 20 wt% solution of sulphuric acid in distilled water and weighed. The impinger is filled with a known volume of distilled water (for all the experiments in this report this was 50 ml). The flow rate through the impinger is set using the MKS mass flow meter and a reading from the nebuliser pump is recorded. At $t=0$ the pump for the nebuliser is started. After one minute the pump for the impinger is then started. This allows time for the aerosol to reach the outlet of the pipe and the impinger now samples over a further five minute period. On stopping measurement, the nebuliser is re-weighed and a final reading taken from the nebuliser pump. From this the flow through the the nebuliser

can be determined. To finish samples are taken from the impinger (50 ml) and the pipe (100 - 150 ml). The concentrations are then determined by titration.

2.2.2 Titration with sodium hydroxide

For the titration experiments, the following equipment is used:

- Metrohm Herisau Potentiograph E536
- Metrohm Herisau Dosimat E535
- Metrohm Herisau pH electrode
- Merck Titrisol 0.1 M NaOH titer

The sulphuric acid concentration in both the impinger and the pipe are determined using the titration setup, which consists of the equipment specified above.

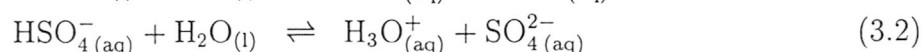
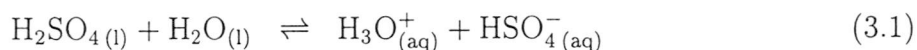
Chapter 3

Measurements

3.1 Theory of measurements

3.1.1 Titration with sodium hydroxide

When sulphuric acid is dissolved in water the following reactions take place:



The equilibrium of the second reaction (equation 3.2) is described by the dissociation constant $K_{\text{HSO}_4^-}$:

$$K_{\text{HSO}_4^-} = \frac{[\text{H}_3\text{O}^+][\text{SO}_4^{2-}]}{[\text{HSO}_4^-][\text{H}_2\text{O}]} \quad (3.3)$$

The terms x and y are used to simplify the calculations. x is the concentration of H_3O^+ and of HSO_4^- in reaction one (equation 3.1). y is the concentration of H_3O^+ and of SO_4^{2-} in reaction two (equation 3.2). As both reactions are in equilibrium, the H_3O^+ term for the dissociation constant must be the sum of the concentration of H_3O^+ from each reaction. Therefore this makes the dissociation constant equal to:

$$K_{\text{HSO}_4^-} = \frac{(x + y)y}{(x - y)} = \frac{y^2 + xy}{x - y} \quad (3.4)$$

Using the technique of titration: sodium hydroxide of known concentration is added to a stirred sample solution at a known rate. The amount of sodium hydroxide required to reach a pH value of 7 is used to determine the total amount of pure acid which is present in the sample. A schematic illustration of a titration curve is shown in Figure 3.1.

This means that the total H_3O^+ concentration in the impinger can be calculated:

$$\frac{V_{\text{NaOH}} C_{\text{titre}}}{V_s} = x + y \quad (3.5)$$

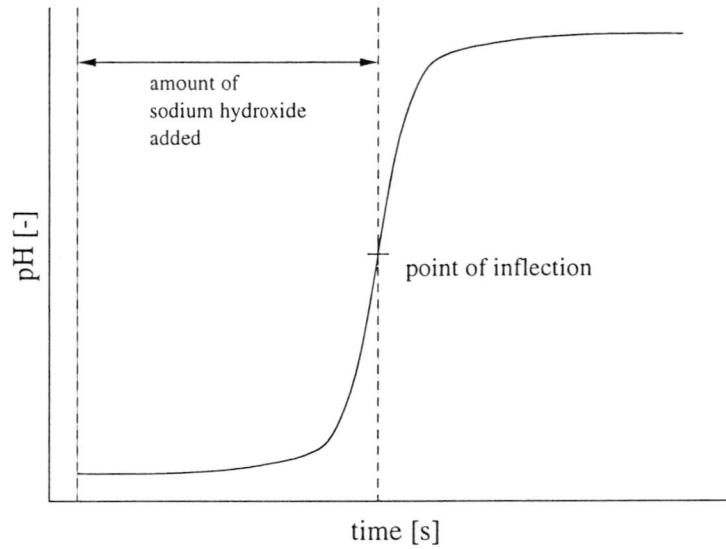


Figure 3.1: Schematic drawing of a titration curve

In which:

V_{NaOH}	sodium hydroxide added	[l]
C_{titre}	sodium hydroxide concentration of the titer	[mol · l ⁻¹]
V_s	volume of the batch sample	[l]

Using $K_{HSO_4^-} = 1.12 \cdot 10^{-2} \text{ mol} \cdot \text{l}^{-1}$ (Weast (1967)), x and y are calculated by combining equations 3.4 and 3.5.

On knowing x the mass concentration of the sulphuric acid sampled is calculated using equation 3.6.

$$C_{imp} = \frac{5 n_{H_2SO_4} V_s M_{acid}}{\phi_{V,imp} t_m} \quad (3.6)$$

In which:

C_{imp}	sampled mass concentration of 20 wt% acid	[g · m ⁻³]
$n_{H_2SO_4}$	amount of pure acid sampled	[mol]
V_s	volume of the batch sample	[l]
M_{acid}	molecular mass of pure sulphuric acid	[g · mol ⁻¹]
$\phi_{V,imp}$	impinger flow rate	[m ³ · s ⁻¹]
t_m	measuring time	[s]

To determine the efficiency the mass concentration of the sulphuric acid droplets formed by the nebuliser must be known. This is found by considering the mass decrease during the experiments and the gas flow rate through the nebuliser:

$$C_{neb} = \frac{\Delta m}{\Delta V \cdot 1.17} \quad (3.7)$$

In which:

C_{neb}	output concentration of the nebuliser	$[g \cdot m^{-3}]$
Δm	mass difference	$[g]$
ΔV	flow rate through the nebuliser	$[m^3 \cdot s^{-1}]$

The above equation has been adjusted for pressure change and flow rate. This adjustment is required as the device for measuring the flow is calibrated for 1 bar. But the actual system pressure is slightly greater due to the nebuliser resistance to the flow. Using the ideal gas law this addition pressure is calculated and for the flow rate of $10 \text{ l} \cdot \text{min}^{-1}$ this was 0.17. Therefore to determine the concentration accurately, a correction factor of 1.17 must be included.

With both the mass concentrations of the impinger and the nebuliser, it is possible now to determine the transfer efficiency:

$$\eta_t = \frac{C_{imp}}{C_{neb}} \cdot 100 \quad (3.8)$$

In which:

η_t	transfer efficiency	$[-]$
----------	---------------------	-------

To get a more accurate value for the efficiency, the amount of acid lost within the pipeline during the experiment must be considered. The amount of acid lost is determined using equations 3.4, 3.5 and 3.9.

$$M_{pipe} = 5 n_{H_2SO_4} V_s M_{acid} \quad (3.9)$$

In which:

M_{pipe}	mass of 20wt% acid within pipeline	$[g]$
$n_{H_2SO_4}$	amount of pure acid sampled	$[mol]$
V_s	volume of the batch sample	$[l]$
M_{acid}	molecular mass of pure sulphuric acid	$[g \cdot mol^{-1}]$

Now the mass difference is adjusted to account for the acid lost in the pipeline ($\Delta m - M_{pipe}$) and this changes the values of C_{neb} and the efficiency respectively.

3.2 Calculation of the minimum detectable concentration

At this present time the M.A.C value for sulphuric acid is $1 \text{ mg} \cdot \text{m}^{-3}$. As it is now believed that sulphuric acid is carcinogenic, a decrease in this value is expected. Therefore it must be known what the minimum value of concentration the impinger can detect. Using ion chromatography this value can be determined. To do this the following assumptions have to be made:

ion chromatography detection limit	1	ng
ion chromatography sampling loop	100	μl
sampling time	5	min

For impinger type, designIIr with the sampling probe attached under optimum conditions of $V_{imp} = 50$ ml and $\phi_{v,imp} = 8.5 - 10 \text{ l} \cdot \text{min}^{-1}$ the minimum detectable concentration is calculated to be between $19 - 22.5 \text{ } \mu\text{g} \cdot \text{m}^{-3}$ (The calculation can be found in Appendix B). Both these values are lower than the current M.A.C value and therefore this impinger designIIr with sampling probe can be used for actual sampling of sulphuric acid aerosol in still air.

Chapter 4

Results

4.1 Expected results

Analysis of previous results suggest that for a certain flow rate, the transfer efficiency has a maximum value. There are two effects which explain this.

1. With increasing flow rate, the collection of the aerosol through inertial impaction becomes more efficient
2. With increasing flow rate, the capture of the aerosol through bubble transfer becomes less efficient due to increase in bubble size.

These two theories can be shown schematically, see Figure 4.1. The lower diagram illustrates both impaction and bubble transfer as a function of the flow rate. By combining these two curves the upper diagram was produced. This curve clearly confirms that we can expect to see a maximum transfer efficiency occurring.

4.2 Original setup

With the original setup no results were actually obtained as the amount of acid caught by the impinger was so insignificant that titrations were not possible.

4.3 Working setup

4.3.1 Differing impinger flow rate

The results obtained with the working setup at different impinger flow rates are given in Table 4.1:

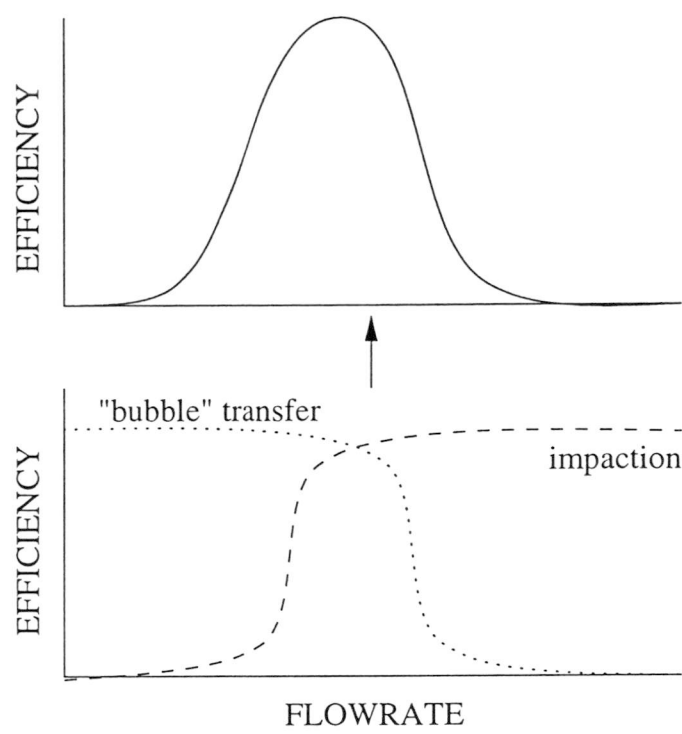


Figure 4.1: Schematic illustration of factors influencing transfer efficiency

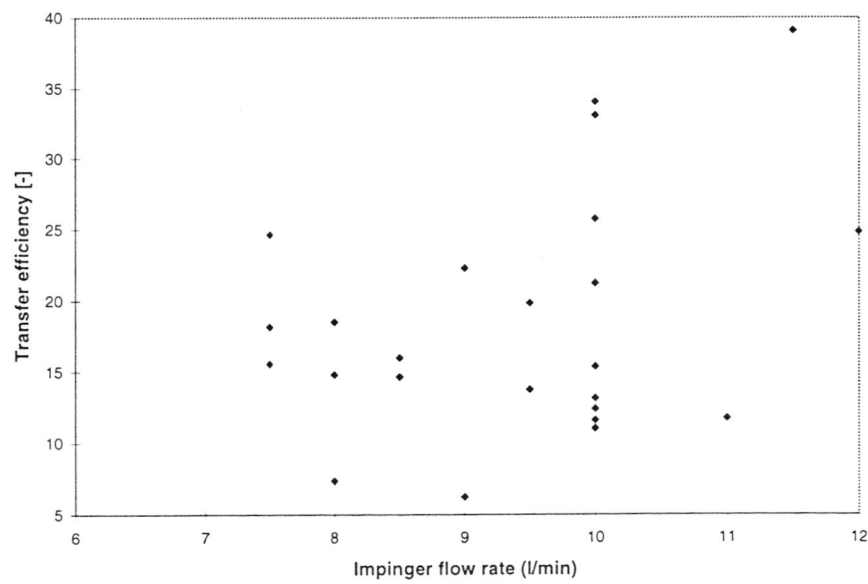


Figure 4.2: Transfer efficiency vs. impinger flow rate ($V_{imp} = 0.5$ l)

Experiment	Δm [g]	ΔV [m ³]	$\phi_{V,imp}$ [l · min ⁻¹]	η_t [%]	M_{pipe} [g]	η_{ta} [%]
8a	1.10	69	7.5	15.636	0.402	24.631
9	1.18	69	7.5	7.503	0.611	15.562
15	1.10	69	7.5	8.638	0.577	18.175
16	1.12	68	8	7.973	0.517	14.816
24	1.34	69	8	6.025	0.245	7.374
26	1.18	69	8	13.665	0.309	18.528
10	1.11	68	8.5	8.474	0.522	16.007
27	1.09	69	8.5	10.667	0.297	14.657
25	1.26	69	9	5.115	0.227	6.236
28	1.06	69	9	14.794	0.357	22.296
11	1.05	67	9.5	9.371	0.555	19.869
14	1.14	68	9.5	7.496	0.520	13.791
6	1.16	70	10	9.320	0.181	11.040
7a	1.19	69	10	9.614	0.269	12.427
7b	1.17	68	10	7.361	0.429	11.622
17	0.98	67	10	13.716	0.585	34.063
19	1.07	68	10	12.749	0.658	33.092
20	0.97	67	10	11.452	0.539	25.747
21	1.09	69	10	13.575	0.394	21.259
22	1.31	69	10	10.463	0.420	15.404
23	1.20	69	10	10.527	0.241	13.167
12	1.03	68	11	8.596	0.277	11.767
18	0.95	67	11.5	15.248	0.579	39.072
8b	1.04	68	12	12.774	0.505	24.845

Table 4.1: Experimental data and transfer efficiency for different impinger flow rates

To consider this data, a graph (Figure 4.2) is drawn of the transfer efficiency against the impinger flow rate. This highlights the great variety in efficiencies at each flow rate, making it difficult to draw any conclusions. For example, taking 10 l · min⁻¹ the efficiency ranges from 11 % to 34 %. An attempt was made at this flow rate to produce a repeatable result but no matter how many experiments were carried out there was no improvement in the results. Also it must be noted that the efficiencies are much lower than those found by Verkoeijen (1997). As explained in the previous section, it was expected that an optimum flow rate would be obtain as this had been found when using a smaller diameter pipeline. But this is not the only change to the setup from the previous study (Verkoeijen (1997)) as there has also been a sampling probe added to the end of the impinger.

4.3.2 Small diameter pipe

There are three possible factors for the scatter in the results:

1. The sampling probe.

2. The acid loss during the experiment.
3. The pipe diameter.

Verkoeijen (1997) carried out the experiments using only an impinger (designIIr) and a smaller diameter pipe (40 mm), finding that it was possible to obtain a repeatable efficiency at one flow rate. Therefore by using this setup but with the sampling probe attached to the impinger it is possible to test whether or not the probe is the reason for the poor results. The experimental results for an impinger flow rate of $10 \text{ l} \cdot \text{min}^{-1}$ are found in Table 4.2. From these values it can be concluded that the transfer efficiency (η_t) is constant at around 55% but when the final transfer efficiency (η_{ta}) is deduced, a scatter in the results appears again. As a constant value for η_t at one flow rate can be shown, the assumption that the sampling probe does not cause the errors is reasonable. This leaves a further two variables that must be checked.

Experiment	Δm [g]	ΔV [m ³]	η_t [%]	M_{pipe} [g]	η_{ta} [%]
29	1.13	69	55.499	0.286	74.281
30	1.05	68	59.669	0.071	64.024
31	0.99	68	76.998	0.061	82.065
32	1.17	69	52.281	0.069	55.582
33	1.13	68	58.762	0.128	66.251

Table 4.2: Experimental data and transfer efficiency with small diameter pipe

4.3.3 Acid loss in pipeline

As suggested in the previous subsection the acid loss may be varying. The value of η_{ta} is related to the amount of acid lost within the pipeline during the experiment and therefore to obtain an accurate value for η_{ta} , the exact amount of acid lost must be known. To be definite about this, only the acid loss within the pipe was determined in the following experiments. To improve the accuracy of the results a larger sample volume of 150ml was taken. Table 4.3 shows the data which is relevant to these experiments. First look at these

Experiment	V_s [l]	M_{pipe} [g]
34	0.15	0.488
35	0.15	0.633
36	0.15	0.447
37	0.15	0.539
38	0.15	0.455
39	0.15	0.397
40	0.15	0.407

Table 4.3: Experimental data for acid loss

values show that there is approximately 50 % variation in the amount of acid lost. This is

incorrect though as there was problems with the titration equipment during experiments 35 and 37. This may have lead to errors in these results and therefore they have been discarded. Looking at the other values of M_{pipe} obtained there is constant value of 0.4 g of acid lost in the experiment. Early indications that the acid loss was not constant can be explained. With previous experiments the sample volume was 100ml and only one end of the pipe was closed tightly, making it difficult to totally wash the pipe of acid. This may have lead to some acid being left within the pipe. Therefore each time the accuracy of the sample could be questioned. For this set of experiments both ends of the pipe were closed. This improvement makes it possible to thoroughly flush the pipeline of acid. Combining this with the larger volume of water, it is now possible to have the acid loss as constant. This is what would be expected anyway.

4.4 Final setup

The previous section shows that the main problem must be with the diameter size of the pipe being used as this is the only other parameter which has been varied from the previous work carried out on this topic. As the aim of this project was to take samples in still air, a solution was to move the position where the impinger sampled.

Firstly it has to be shown that the acid loss with this new setup is also constant as predicted earlier. This is found in the same way as for the working setup. Due to some inconsistencies in the mass difference from the nebuliser, the acid loss on occasions was found to be greater than the amount sprayed. Obviously this is not possible. To overcome this problem, the acid loss within the pipeline was calculated as a percentage of the mass difference in the nebuliser. The amount of acid lost was found to be 0.6 g. This is consistent with the previous setup as the pipeline is longer with the T-junction, so more acid loss was anticipated. So instead of sampling the acid loss each time, it is taken as 60 % of the mass difference for that particular experiment, since Δm is approximately 1 g each time.

Experiment	Δm [g]	ΔV [m ³]	$\phi_{V,imp}$ [l · min ⁻¹]	η_t [%]	M_{pipe} [g]	η_{ta} [%]
53	1.13	69	7.5	14.277	0.678	35.693
54	1.03	68	8.5	16.040	0.618	40.102
55	0.97	68	10	28.011	0.582	70.028
56	1.13	68	11	17.242	0.678	43.104
57	1.10	68	7.5	19.491	0.660	48.727
58	1.03	68	8.5	21.064	0.618	52.660
59	1.08	68	10	20.647	0.648	51.618
60	1.20	69	11	16.808	0.720	42.019

Table 4.4: Experimental data and transfer efficiency at different impinger flow rates

For this section the experiments were taken in sets of four. Within each set of results there is four different flow rates tested. For each set of experiments a graph of the results (see Table 4.4) was plotted.

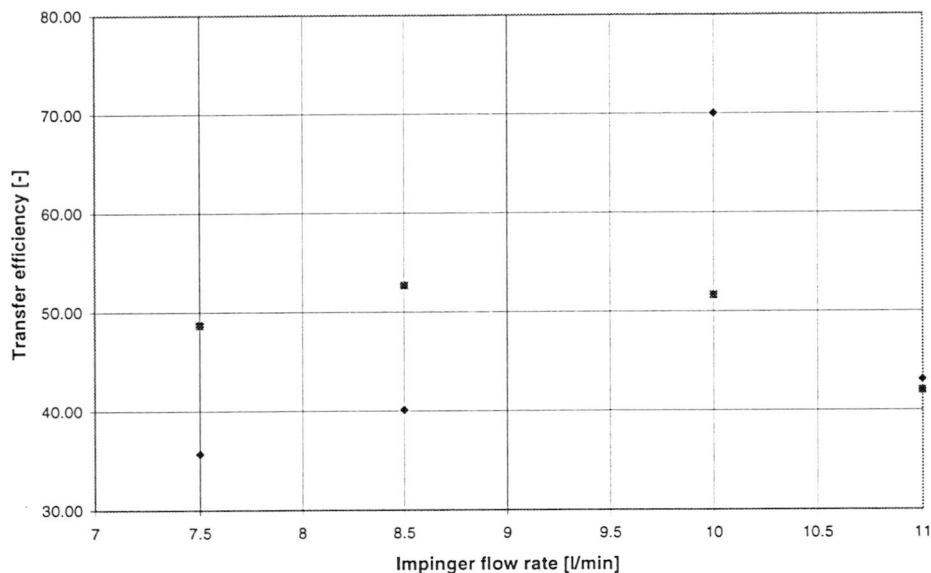


Figure 4.3: Transfer efficiency vs. impinger flow rate, ($V_{imp} = 0.5$ l). Both series of experiments under the same conditions. The diamonds represent experiment set 1 and the squares represent experiment set 2

Looking at these graphs, each shows the same and expected trend of an initial increase in transfer efficiency to an optimum value and then a decrease in the efficiency after that point. Although the problem is that both the graphs do not peak at the same value. The experiment proves though that the sampling probe can sample in still air conditions but more experiments are needed to give a definite value of which impinger flow rate to operate at.

Chapter 5

Growth

The aim of this project is to accurately measure sulphuric acid concentration in still air. Since sulphuric acid is hygroscopic it tends to grow in a humid environment. Therefore this growth must be known for the measurements to be accurate.

A model has been created based on the thermodynamic equilibrium between a sulphuric acid aerosol droplet and its surroundings. This model considers how the growth factor, f_g and the growth time t_g will influence any measurements.

The model has been tested experimentally using an acoustic levitator. This allows the observation of the droplet by a calibrated microscope as the relative humidity changes. The relative humidity calculated by the model where no grow of the droplet for that specific acid concentration is set before the droplet is introduced by a microlitre syringe into the levitator. The droplet is observed to see if the diameter remains constant before the relative humidity is changed and the grow monitored.

The results of three different acid concentrations show agreement in the growth factor with those determined by the model. With the growth times the experimental values relate to the theoretical values at low humidities but not with high humidities. Therefore the model can be used to give an indication of the growth times but can easily be used to predict the growth factors of the droplets. For further details see Appendix C which includes the paper as it will be submitted to Aerosol Science & Technology.

Chapter 6

Conclusions

A setup has been built to simulate still air conditions for a sulphuric acid aerosol with a known concentration. The measurement of concentration of sulphuric acid in an aerosol in still air conditions can be achieved using the sampling probe designed by (Verkoeijen (1997)). The optimum flow rate of impinger type designIIr with a sampling probe attached is in the range of $8.5 - 10 \text{ l} \cdot \text{min}^{-1}$. The sampling time is five minutes and the impinger volume $V_{imp} = 50 \text{ ml}$. Assuming the ion chromatography detection limit of 1 ng and a sampling loop volume of $100 \mu\text{l}$ the minimum detectable concentration is calculated to be between $19 - 22.5 \mu\text{g} \cdot \text{m}^{-3}$. It has been shown that impinger designIIr can be used to sample unknown acid concentrations in still air with a transfer efficiency of 50% and an impinger flow rate between $8.5 - 10 \text{ l} \cdot \text{min}^{-1}$ compared with a transfer efficiency of 56% and a flow rate of $10 \text{ l} \cdot \text{min}^{-1}$ determined by (Verkoeijen (1997)). Overall the transfer efficiencies obtained are lower than those achieved by (Verkoeijen (1997)). The acid lost in the pipeline during the experiment is 60% of the aerosol produced in the nebuliser. The final setup can be used to calibrate the transfer efficiency of different impingers in still air.

A simple model which predicts the growth of sulphuric acid in varying relative humidities has been developed. The accuracy of this model in terms of growth factor is to within 10% . The model can only make a prediction of the growth times with increasing accuracy at lower relative humidities.

Chapter 7

Recommendations

- An accurate value for the optimum impinger flow rate should be determined by further experimental work using the final setup.
- The flow rate through the nebuliser should be varied to see if this affects the transfer efficiency of impinger as so far only the one flow rate has been used.
- The concentration of the acid within the nebuliser could be changed to determine whether similar results are obtained at each concentration.
- The aerosol concentration should be changed by for instance adding dilution air or turning the nebuliser pump on and off.
- The humidities set within the levitator should be monitored during the experiment to determine the accuracy of the air conditioning system.
- There is some doubt to whether a high humidity is possible with this setup as when the droplet is inserted into its equilibrium relative humidity it is expected that may either grow or shrink rather than always shrinking. Therefore it must be checked if 100 % has been achieved.
- To improve the accuracy of the results the calibrated microscope should be replaced with a video camera. For example it could be set to take pictures every ten seconds. This would enable the use of a standard image analysis program on the computer such as image tool or optimus to determine the droplet diameter.
- Higher acid concentrations could be tested to determine whether the model is accurate at these concentrations as well.
- The particle size should be varied over a wider range since so far only 1 - 2 μm have been tested and if the model is to be used for aerosols then smaller particle sizes will need to be tried.

Bibliography

- Clegg, S. and Brimblecombe, P. (1995). Application of a multicomponent thermodynamic model to activities and thermal properties of 0-40 mol·kg⁻¹ aqueous sulfuric acid from <200 to 328 K. *J. Chem. Eng. Data*, **40**, 43-64.
- Coulson, J. and Richardson, J. (1990). *Chemical Engineering Vol 1. Fluid flow, heat transfer and mass transfer*. Pergamon, Oxford.
- Hinds, W. (1982). *Aerosol technology: properties, behavior, and measurement of airborne particles*. John Wiley and Sons.
- Janssen, L. and Warmoeskerken, M. (1991). *Transport Phenomena Data Companion*. Delftse Uitgevers Maatschappij B.V.
- Khlystov, A., Ten Brink, H., and Wijers, G. (1993). Hygroscopic growth rates of aerosols at high relative humidity. Technical Report ECN-C-93-011, ECN.
- Massucci, M., Clegg, S., and Brimblecombe, P. (1996). Equilibrium vapor pressure of H₂O above aqueous H₂SO₄ at low temperature. *J. Chem. Eng. Data*, **41**, 765-778.
- Smith, J. and Van Ness, H. (1987). *Introduction to chemical engineering thermodynamics*. McGraw-Hill International, fourth edition.
- Timmermans, J. (1960). *The physico-chemical constants of binary systems in concentrated solutions*. Interscience Publishers, Inc., New York.
- Verkoeijen, D. (1997). *The development of a sulfuric acid aerosol monitor*. Master's thesis, Delft University of Technology.
- Weast, R., editor (1967). *Handbook of Chemistry and Physics*. The Chemical Rubber Co., Cleveland, OH, 48th edition.

Appendix A

Example Calculations

A.1 Titration experiments

A.1.1 Impinger sample

Mass:	Gas meter:
108.78 g	116 l
107.71 g	184 l
$\Delta m = 1.07 \text{ g}$	$\Delta V = 68 \text{ l}$

$$t_m = 5 \text{ min}$$

$$V_{NaOH} = 2.9 \text{ ml}$$

$$V_s = 50 \text{ ml}$$

$$C_{titre} = 0.1 \text{ mol} \cdot \text{l}^{-1}$$

Calculate $x + y$ from equation 3.5:

$$x + y = \frac{2.9 \cdot 10^{-3} \cdot 0.1}{0.05} = 0.0058 \text{ mol} \cdot \text{l}^{-1}$$

$$x = 0.0058 - y$$

By combining this with equation 3.4, x and y can be calculated:

$$y = \frac{1.12 \cdot 10^{-2} \cdot 0.0058}{0.0058 + (2 \cdot 1.12 \cdot 10^{-2})} = 0.0023 \text{ mol} \cdot \text{l}^{-1}$$

$$x = 0.0058 - 0.0023 = 0.0035 \text{ mol} \cdot \text{l}^{-1}$$

Calculate C_{imp} using equation 3.6:

$$C_{imp} = \frac{5 \cdot 0.0035 \cdot 0.05 \cdot 98.08}{10 \cdot 5 \cdot 10^{-3}} = 1.715 \text{ g} \cdot \text{m}^{-3}$$

Determine C_{neb} from equation 3.7:

$$C_{neb} = \frac{(108.78 - 107.71)}{(184 - 116) \cdot 1.17 \cdot 10^{-3}} = 13.45 \text{ g} \cdot \text{m}^{-3}$$

The transfer efficiency is therefore (using equation 3.8):

$$\eta_t = \frac{1.715}{13.45} \cdot 100 = 12.75 \%$$

A.1.2 Acid loss sample

$$V_{NaOH} = 18.475 \text{ ml}$$

$$V_s = 100 \text{ ml}$$

$$C_{titre} = 0.1 \text{ mol} \cdot \text{l}^{-1}$$

Calculate $x + y$ from equation 3.5:

$$x + y = \frac{18.475 \cdot 10^{-3} \cdot 0.1}{0.1} = 0.018475 \text{ mol} \cdot \text{l}^{-1}$$

$$x = 0.018475 - y$$

By combining this with equation 3.4, x and y can be calculated:

$$y = \frac{1.12 \cdot 10^{-2} \cdot 0.018475}{0.018475 + (2 \cdot 1.12 \cdot 10^{-2})} = 0.005062 \text{ mol} \cdot \text{l}^{-1}$$

$$x = 0.018475 - 0.005062 = 0.013413 \text{ mol} \cdot \text{l}^{-1}$$

Calculate M_{pipe} using equation 3.9.

$$M_{pipe} = 5 \cdot 0.013413 \cdot 0.1 \cdot 98.08 = 0.658 \text{ g}$$

Calculate C_{neb} using adjusted mass difference:

$$C_{neb} = \frac{(1.07 - 0.658)}{68 \cdot 1.17 \cdot 10^{-3}} = 5.18 \text{ g} \cdot \text{m}^{-3}$$

The adjusted transfer efficiency is therefore:

$$\eta_{ta} = \frac{1.715}{5.18} \cdot 100 = 33.09 \%$$

Appendix B

Calculation of the minimum detectable concentration

ion chromatography detection limit	1	ng
ion chromatography sampling loop	100	μl
sampling time	5	min
impinger volume	50	ml
impinger flow rate	8.5-10	$\text{l} \cdot \text{min}^{-1}$
transfer efficiency	0.5266	

The concentration of sulfate (and thus of sulphuric acid) in the sampling loop is calculated by dividing the ion chromatography detection limit by the volume of the sampling loop:

$$[\text{H}_2\text{SO}_4] = \frac{1 \cdot 10^{-9}}{100 \cdot 10^{-6}} = 1 \cdot 10^{-5} \text{ g} \cdot \text{l}^{-1}$$

Using this concentration, the mass of sulphuric acid in the impinger can be calculated:

$$m_{\text{H}_2\text{SO}_4} = V_{\text{imp}}[\text{H}_2\text{SO}_4] = 50 \cdot 10^{-3} \cdot 1 \cdot 10^{-5} = 5 \cdot 10^{-7} \text{ g}$$

The minimum detectable concentration is calculated by dividing the mass of sulphuric acid by the volume of air sampled, and taking the transfer efficiency into account. As each flow rate has its own relating transfer efficiency, then a decision to which efficiency to use in the calculation must be made. For this calculation the lower of the two possible transfer efficiencies is chosen:

$$C_{md} = \frac{m_{\text{H}_2\text{SO}_4}}{t_m \phi_{V, \text{imp}} \eta_t} = \frac{5 \cdot 10^{-7}}{5 \cdot 8.5 \cdot 10^{-3} \cdot 0.5266} = 22.34 \cdot 10^{-6} \text{ g} \cdot \text{m}^{-3}$$

$$C_{md} = \frac{m_{\text{H}_2\text{SO}_4}}{t_m \phi_{V, \text{imp}} \eta_t} = \frac{5 \cdot 10^{-7}}{5 \cdot 10 \cdot 10^{-3} \cdot 0.5266} = 18.99 \cdot 10^{-6} \text{ g} \cdot \text{m}^{-3}$$

Appendix C

Growth

The growth of H_2SO_4 , model and experiments

D. Verkoeijen¹ # W. Oostra* A. McIntyre*
H. van der Kooij² J.C.M. Marijnissen* B. Scarlett*

April 14, 1997

¹Delft University of Technology, Department of Chemical Engineering and Material Sciences,
Particle Technology Group

²Delft University of Technology, Department of Chemical Engineering and Material Sciences,
Thermodynamic Group (?)

Abstract

In this article, a simple model is presented which describes the growth of H_2SO_4 in a humid environment. The model uses easily available data from literature and calculates the growth as a function of the relative humidity and of the droplet's H_2SO_4 concentration. Assuming diffusive mass transfer, the model also gives an indication of growth times. Finally, experiments to support the model, for H_2SO_4 concentrations up to 31wt%, are reported.

C.1 Introduction

Aerosols containing salts, sulfates or nitrates are hygroscopic and therefore tend to grow in a humid environment. This growth can become a problem when this aerosol needs to be measured. Two factors may influence the results, growth factor and growth time. The growth factor f_g is defined as the ratio of the diameter after growth to the initial diameter. The growth time t_g is defined as the time needed to reach the final diameter. Several models have been reported in literature describing the growth of salts (Clegg and Brimblecombe (1995) and Khlystov *et al.* (1993)), however a model which enables calculation of growth factors and times of a model H_2SO_4 aerosol is not yet available. In this article we present a simple model based on the thermodynamic equilibrium between an aerosol droplet and its environment. The validity of the model is checked against experimental data, obtained using an acoustic levitator. In the experiments a H_2SO_4 -water droplet is placed in an acoustic levitator, enabling the observation of the droplet as the relative humidity changes.

C.2 Theory

In the model, the phenomenon of 'growth' is seen as the transport of water from the air to the droplet. Driven by a concentration gradient, water diffuses from the air to the droplet. All the resistance to mass transfer is combined in a 'boundary layer' and the droplet itself is assumed to be an ideally stirred system.

C.2.1 Water concentration in the air

The first step in calculating the growth of sulfuric acid droplets is the determination of the concentration of water vapor in the air, which is a function of the humidity. In calculating the dependency of the water vapor concentration on the humidity we follow Coulson and Richardson (1990).

The humidity of a gas is defined as the mass of water vapor per unit mass of dry gas and is given by:

$$\mathcal{H} = \frac{P_w}{P - P_w} \left(\frac{M_w}{M_{air}} \right) \quad (C.1)$$

With:

\mathcal{H}	humidity	$[\text{kg} \cdot \text{kg}^{-1}]$
P	pressure	$[\text{Pa}]$
P_w	partial vapor pressure	$[\text{Pa}]$
M_w	molecular mass of water	$[\text{kg} \cdot \text{mol}^{-1}]$
M_{air}	molecular mass of air	$[\text{kg} \cdot \text{mol}^{-1}]$

The humidity of the gas when it is saturated with water vapor at a given temperature is given by:

$$\mathcal{H}_0 = \frac{P_{w0}}{P - P_{w0}} \left(\frac{M_w}{M_a} \right) \quad (C.2)$$

With:

\mathcal{H}_0	humidity of saturated gas	$[\text{kg} \cdot \text{kg}^{-1}]$
P_{w0}	saturated partial vapor pressure	$[\text{Pa}]$

The percentage humidity is defined as $100\mathcal{H}/\mathcal{H}_0$. The percentage relative humidity RH is given by:

$$RH = 100 \frac{P_w}{P_{w0}} \quad (C.3)$$

Combining equations C.1, C.2, and C.3 leads to:

$$\frac{C_{H_2O}}{\rho_{air} - C_{H_2O} \left(\frac{M_{air}}{M_w} \right)} = \mathcal{H} = \frac{P_{w0}}{P - \frac{RH P_{w0}}{100}} \left(\frac{M_w}{M_a} \right) \left(\frac{RH}{100} \right) \quad (C.4)$$

In which C_{H_2O} is the water concentration and ρ_{air} is the density of air.

The saturated partial vapor pressure at $T=298$ K and $P=1$ bar is equal to 3166 Pa (Smith and Van Ness (1987)). Using $M_w=18 \cdot 10^{-3}$ and $M_{air}=28.9 \cdot 10^{-3} \text{ kg} \cdot \text{mol}^{-1}$, equation C.1 is transformed to:

$$\mathcal{H} = 19.7190 \frac{RH}{10^5 - 31.66 RH} \quad (C.5)$$

Combining equation C.5 and equation C.4 gives the required relationship for the concentration of water in the air as a function of the relative humidity:

$$C_{H_2O} = \frac{\rho_{air} \mathcal{H}}{1 + 1.6056 \mathcal{H}} = \frac{19.7190 \rho_{air} \frac{RH}{10^5 - 31.66 RH}}{1 + 1.6056 \left(19.7190 \frac{RH}{10^5 - 31.66 RH} \right)} \quad (C.6)$$

C.2.2 Calculation of equilibrium acid concentration in the droplet

The equilibrium acid concentration in the droplet can be calculated by setting the water concentration in the air equal to the water concentration in the ‘boundary layer’ around the droplet. The concentration of water above a flat liquid surface is determined by the vapor pressure (equation C.7).

$$C_{H_2O,bl} = \frac{M_w P_w}{R T} \quad (C.7)$$

Because liquid aerosol particles have a curved surface, a greater partial pressure is required to maintain mass equilibrium at a given temperature than for a flat liquid surface. This required increase in the partial vapor pressure, known as the Kelvin effect, increases with decreasing particle size. Calculation of the Kelvin effect for sulfuric acid droplets shows that it may be neglected for particles larger than 50 nm. The particles for which the model is developed are clearly larger than 50 nm, subsequently the Kelvin effect is not taken into account.

In the past, the vapor pressure of the sulfuric acid–water system has been studied extensively. Using data from three independent studies (Timmermans (1960) (first two) and Massucci *et al.* (1996)), a vapor pressure vs. acid concentration curve at $T = 298$ K was constructed (Figure C.1).

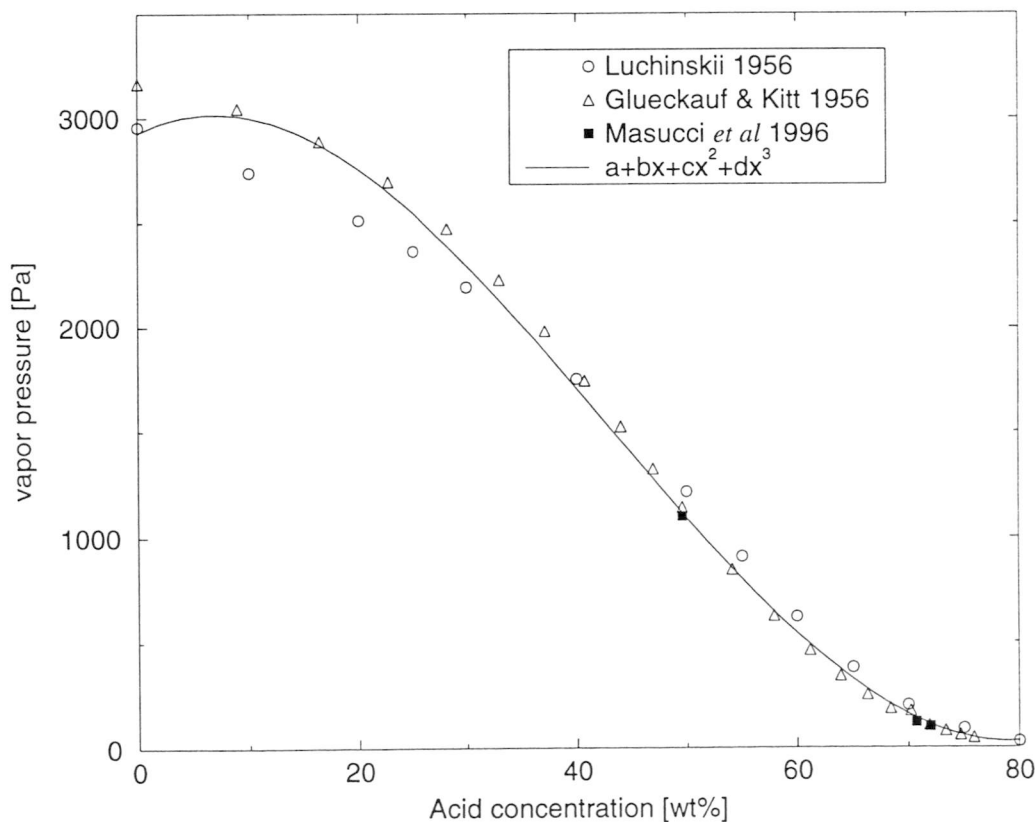


Figure C.1: Vapor pressure vs. sulfuric acid concentration

To ease the use of the data in further calculations a data-fit was made. The resulting cubic function is given below. C_d is the acid concentration in the droplet in wt%.

$$P_w = 2930 + 26C_d - 2.05C_d^2 + 15.9 \cdot 10^{-3}C_d^3 \quad (\text{C.8})$$

Setting the water concentration in the boundary layer $C_{H_2O,bl}$ equal to the water concentration in the bulk air C_{H_2O} gives the equilibrium acid concentration in the droplet as a function of the relative humidity.

C.2.3 Calculation of growth factor

From the sulfuric acid equilibrium concentrations vs. relative humidity data the growth factor at different initial acid concentrations can be calculated.

Initially, the total volume of the droplet is $V_{0,tot}$ and the volume of sulfuric acid in the droplet is $V_{0,a}$.

$$V_{0,tot} = \frac{\pi}{6}d_{p0}^3 \quad (\text{C.9})$$

$$V_{0,a} = V_{0,tot} \frac{\frac{C_0}{\rho_a}}{\frac{C_0}{\rho_a} + \frac{100-C_0}{\rho_w}} \quad (\text{C.10})$$

With:

$V_{0,tot}$	total volume	$[\text{m}^3]$
$V_{0,a}$	volume of sulfuric acid	$[\text{m}^3]$
d_{p0}	initial particle diameter	$[\text{m}]$
C_0	initial sulfuric acid concentration	$[\text{wt}\%]$
ρ_a	density of sulfuric acid	$[\text{kg} \cdot \text{m}^{-3}]$
ρ_w	density of water	$[\text{kg} \cdot \text{m}^{-3}]$

In the situation after growth the total volume of the droplet has changed to $V_{1,tot}$, while the volume of sulfuric acid in the droplet has remained the same.

$$V_{1,tot} = \frac{\pi}{6}d_{p1}^3 \quad (\text{C.11})$$

$$V_{1,a} = V_{0,a} = V_{1,tot} \frac{\frac{C_{eq}}{\rho_a}}{\frac{C_{eq}}{\rho_a} + \frac{100-C_{eq}}{\rho_w}} \quad (\text{C.12})$$

With:

$V_{1,tot}$	total volume after growth	$[\text{m}^3]$
$V_{1,a}$	volume of sulfuric acid after growth	$[\text{m}^3]$
d_{p1}	particle diameter after growth	$[\text{m}]$
C_{eq}	sulfuric acid equilibrium concentration	$[\text{wt}\%]$

The equations as given above do not take the mixing volume into account. When it is taken into account the precision of the results increases, by less than 0.5%, while at the

same time the calculations become more complicated. The mixing volume is therefore neglected.

By combining equations C.10 and C.12, the growth factor f_g can now be calculated:

$$f_g = \frac{d_{p1}}{d_{p0}} \quad (\text{C.13})$$

$$= \left(\frac{V_{1,tot}}{V_{0,tot}} \right)^{1/3} \quad (\text{C.14})$$

$$= \left(\frac{C_0(\rho_w C_{eq} + \rho_a(100 - C_{eq}))}{C_{eq}(\rho_w C_0 + \rho_a(100 - C_0))} \right)^{1/3} \quad (\text{C.15})$$

C.2.4 Calculation of growth time

The diffusion of water from the air to the sulfuric acid particle can be described by the following mass balance:

$$\frac{d(\rho_d V)}{dt} = -kA(C_{H_2O,bl} - C_{H_2O}) \quad (\text{C.16})$$

With:

ρ_d	droplet density	$[\text{kg} \cdot \text{m}^{-3}]$
V	droplet volume	$[\text{m}^3]$
t	time	$[\text{s}]$
k	mass transfer coefficient	$[\text{m} \cdot \text{s}^{-1}]$
A	droplet surface area	$[\text{m}^2]$
$C_{H_2O,bl}$	water concentration in 'boundary layer'	$[\text{kg} \cdot \text{m}^{-3}]$
C_{H_2O}	water concentration in air	$[\text{kg} \cdot \text{m}^{-3}]$

The mass transfer coefficient is given by:

$$k = \frac{Sh\mathcal{D}}{d_p} \quad (\text{C.17})$$

In which \mathcal{D} is the diffusion coefficient of water in air ($26.6 \cdot 10^{-6} \text{ m}^2 \cdot \text{s}^{-1}$), d_p is the droplet diameter [m], and Sh is the Sherwood number.

The Sherwood number is a dimensionless mass transfer parameter which relates the total mass transfer to the mass transfer by diffusion. It is dependent on the shape of the particles and the flow regime around them. For spherical particles:

- no flow around the particle: $Sh=2$.
- forced flow around the particle, the Sherwood number is given by equation C.18, in which Re is the Reynolds Number and Sc is the Schmidt number (Janssen and Warmoeskerken (1991)).

$$Sh = 2.0 + 0.66Re^{0.5}Sc^{0.33} \quad (\text{C.18})$$

Combining equations C.19 and C.20, the density of the droplet is rewritten as a function of total particle volume.

$$\rho_d = \frac{\rho_a V_a + \rho_w V_w}{V_a + V_w} \quad (\text{C.19})$$

$$V = V_a + V_w \quad (\text{C.20})$$

$$\rho_d = \frac{(\rho_a - \rho_w)V_a + \rho_w V}{V} \quad (\text{C.21})$$

Assuming a constant value of Sh during the experiment, equation C.16 can now be simplified:

$$d_p d(d_p) = - \frac{2Sh\mathcal{D}(C_{H_2O,bl} - C_{H_2O})}{\rho_w} dt \quad (\text{C.22})$$

Integration of equation C.22 from the initial state ($t=0$; $d_p = d_{p0}$) to the situation at $t = t_g$ (with $d_p = d_{p1}$) leads to a relation for the growth time:

$$\int_{d_{p0}}^{d_{p1}} d_p d(d_p) = \int_0^{t_g} - \frac{2Sh\mathcal{D}(C_{H_2O,bl} - C_{H_2O})}{\rho_w} dt \quad (\text{C.23})$$

$$t_g = - \frac{(d_{p1}^2 - d_{p0}^2)\rho_w}{4Sh\mathcal{D}(C_{H_2O,bl} - C_{H_2O})} \quad (\text{C.24})$$

The water concentration in the boundary layer is averaged over the growth time and calculated from equations C.7 and C.8 with $C_d = (C_0 + C_{eq})/2$.

C.3 Experiments

C.3.1 Experimental setup

The setup used to perform the growth experiments consists of two separate sections. In the first section, shown schematically in Figure C.2, pressurized air with a specific value of the relative humidity is produced by mixing known amounts of dry ($RH=0\%$) and wet ($RH=100\%$) air. Air is dried using a dryer which combines a molecular sieve 5A with silica drying material. The air is humidified in the humidification section by leading it through three heated washing bottles.

The conditioned air is led to a Dantec ultrasonic levitator model 13D10, shown in Figure C.3. Droplets placed in the levitator are watched using a calibrated microscope.

C.3.2 Experimental procedure

Experiments to determine the growth of sulfuric acid droplets were performed as follows:

1. Using growth factor vs. relative humidity and initial acid concentration calculations (as described in Section C.2) the value of the relative humidity RH_{eq} for which a droplet of a specific initial acid concentration C_0 will not grow is determined.

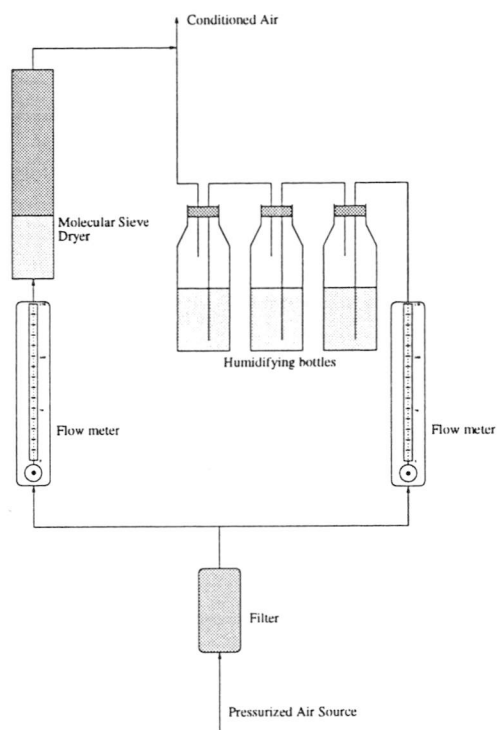


Figure C.2: Experimental setup: air conditioning system

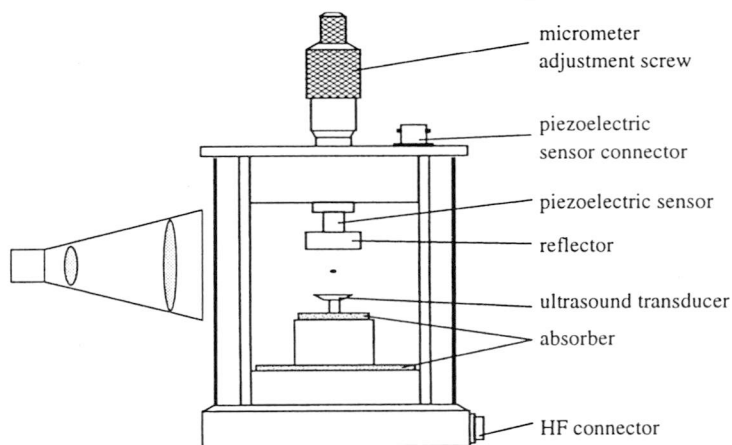


Figure C.3: Experimental setup: levitator and microscope

2. Air is humidified in the humidifying section to RH_{eq} using the two flow meters.
3. Using a microliter syringe, a droplet with an initial acid concentration C_0 is introduced in the levitator.
4. It is observed whether the droplet's diameter d_{p0} remains the same and subsequently the relative humidity is changed to a new value RH_{new} .
5. The growth of the droplet is observed in time.

RH_{new} [%]	$d_{p,0}$ [mm]	f_g [-]	t_g [s]	RH_{new} [%]	$d_{p,0}$ [mm]	f_g [-]	t_g [s]
0	1.632	0.5	750	95	2.208	0.913	480
0	1.584	0.455	1080	95	1.68	0.971	300
0	2.016	0.452	1860	95	1.632	0.971	300
25	1.584	0.515	1500	95	1.632	0.971	390
25	1.632	0.529	960	95	1.68	0.971	360
50	1.584	0.727	510	95	1.632	0.971	300
50	1.632	0.588	840	95	1.68	0.971	150
50	1.968	0.585	1800	95	1.68	0.971	210
75	1.968	0.537	1800	95	1.92	1.025	360
75	1.824	0.618	3600	95	2.16	0.956	480
75	1.68	0.629	3300	95	2.064	0.884	720
95	2.016	0.976	180	95	1.824	0.921	720

Table C.1: Experimental parameters; $C_0=7.7\text{wt}\%$

RH_{new} [%]	$d_{p,0}$ [mm]	f_g [-]	t_g [s]	RH_{new} [%]	$d_{p,0}$ [mm]	f_g [-]	t_g [s]
0	1.584	0.636	870	85	1.584	0.970	240
0	1.488	0.613	1080	85	1.584	0.970	360
0	1.92	0.65	n.a.	85	1.68	0.971	330
25	1.536	0.719	660	85	1.536	0.969	240
25	1.536	0.719	660	85	1.584	0.970	210
25	1.92	0.713	n.a.	85	1.584	0.939	480
50	1.488	0.774	900	85	1.536	0.969	270
50	1.536	0.781	810	85	1.584	0.970	330
50	1.92	0.8	1800	85	1.92	1.0	n.a.

Table C.2: Experimental parameters; $C_0=19.8\text{wt}\%$

The experiments were performed using three different initial acid concentrations: 7.7, 19.8 and 31.0 wt% respectively. The concentration of the H_2SO_4 acid was checked by titration.

Experimental parameters of the different experiments are shown in Table C.1, Table C.2, and Table C.3. The values of the equilibrium relative humidity were the same for each set of experiments: $RH_{eq}=95\%$ for $C_0=7.7\text{wt}\%$, $RH_{eq}=85\%$ for $C_0=19.8\text{wt}\%$, and $RH_{eq}=75\%$ for $C_0=31\text{wt}\%$.

C.4 Results and discussion

Figure C.4 shows the growth factor of sulfuric acid droplets as a function of the relative humidity, for different values of the initial acid concentration. The lines represent the theoretical values, as calculated from the model, while the points represent the experimental data. The experimental points are an average of a number of measurements with different initial droplet sizes ranging from 1.49 to 2.21 mm. The error bars indicate the

RH_{new} [%]	$d_{p,0}$ [mm]	f_g [-]	t_g [s]	RH_{new} [%]	$d_{p,0}$ [mm]	f_g [-]	t_g [s]
0	1.776	0.716	840	75	1.824	0.977	1080
0	1.776	0.716	600	75	1.872	0.974	360
0	1.92	0.775	3000	75	1.872	0.974	300
25	1.776	0.838	510	75	1.824	1.0	n.a.
25	1.776	0.838	480	75	1.824	0.974	360
25	1.92	0.838	2400	75	1.824	0.974	360
50	1.824	0.921	210	75	1.824	0.974	420
50	1.824	0.921	300	75	1.872	0.974	180
50	1.92	0.925	1200	75	2.016	0.952	120

Table C.3: Experimental parameters; $C_0=31.0\text{wt}\%$

95% confidence interval.

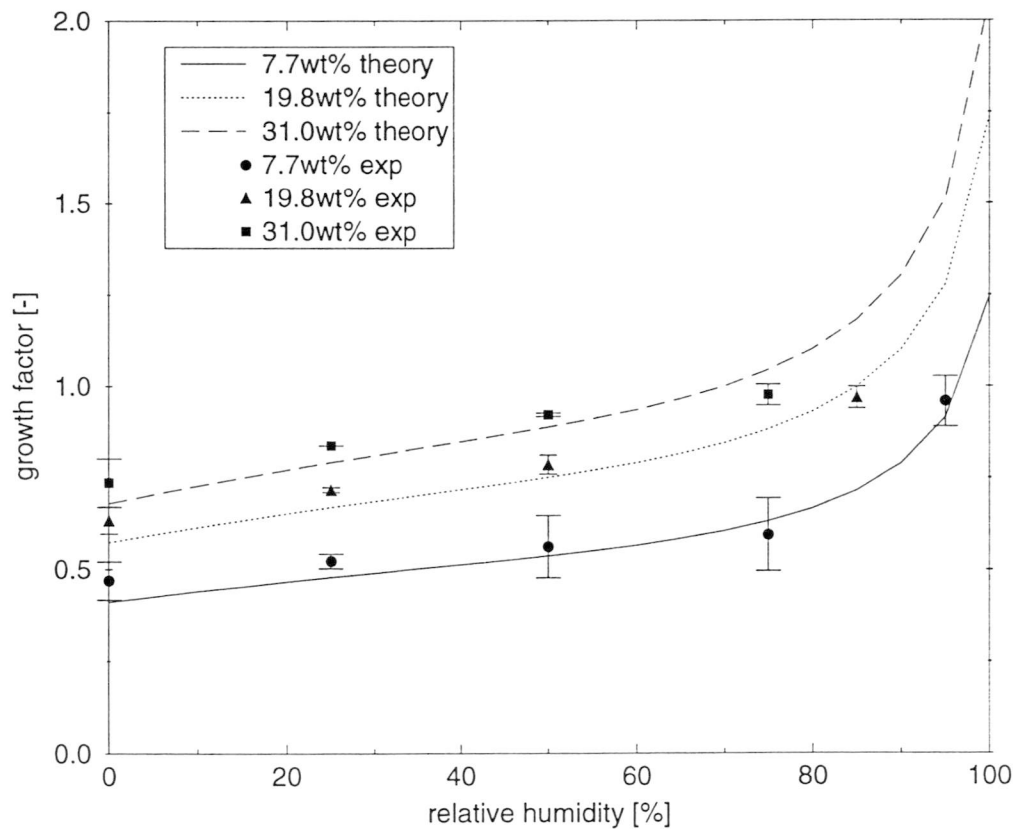


Figure C.4: Growth factor vs. relative humidity

Figure C.5 shows the growth times for different values of RH_{new} . The theoretical growth times are plotted on the y-axis, while the experimental growth times are plotted on the x-axis. The model both overestimates and underestimates the growth times. A possible explanation for the overestimation is the fact that the growth times were calculated using $Sh=2$, while in the experiment an air flow of approximately $1\text{ l} \cdot \text{min}^{-1}$ was led through

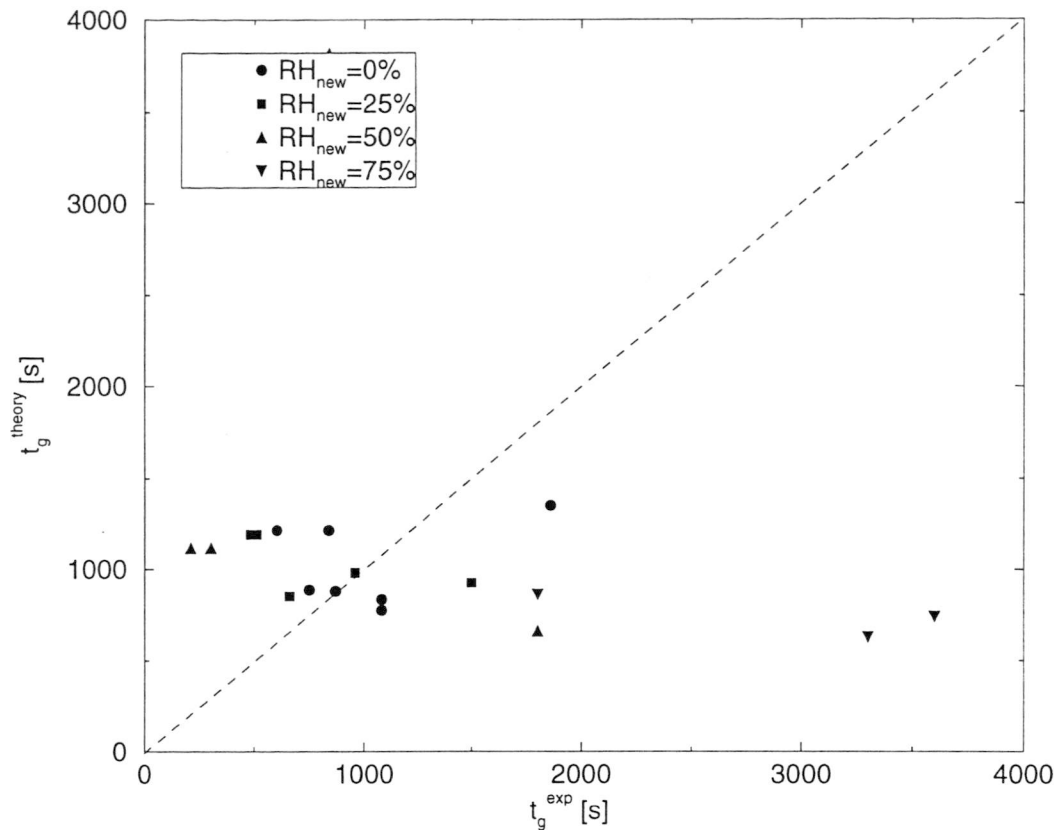


Figure C.5: Theoretical vs. experimental growth time

the levitator. Underestimation can be partly explained by the ‘dead time’, the time that exists between setting RH_{new} in the humidification section and reaching this value of RH_{new} in the levitator. Furthermore , the assumption of an ideally stirred system may not hold true.

C.5 Conclusions

A simple model describing the growth of H_2SO_4 in a humid environment was developed. The model predicts the growth factor to within 10%. However, the predicted growth times are only indicative due to unknown causes.